Journal of Thermal Stresses

ISSN: 0149-5739 (Print) 1521-074X (Online) Journal homepage: www.tandfonline.com/journals/uths20

Effect of temperature on tensile, compressive, and shear strengths of composites

Victor Birman

To cite this article: Victor Birman (15 Apr 2025): Effect of temperature on tensile, compressive, and shear strengths of composites, Journal of Thermal Stresses, DOI: 10.1080/01495739.2025.2485471

To link to this article: https://doi.org/10.1080/01495739.2025.2485471

Published online: 15 Apr 2025.

JOURNAL OF THERMAL STRESSES
https://doi.org/10.1080/01495739.2025.2485471

Taylor & Francis
Taylor & Francis Group

Effect of temperature on tensile, compressive, and shear strengths of composites

Victor Birman

Professor Emeritus of Mechanical Engineering, Missouri University of Science and Technology, Rolla, Missouri, USA

ABSTRACT

The paper is concerned with the prediction of longitudinal and transverse tensile and compressive strengths as well as the in-plane shear strength of a fiber-reinforced composite material subject to an elevated temperature. Additionally, the effect of temperature on the tensile strength of particulate composites is considered. The premise is that since the longitudinal compressive, transverse and shear strengths of uniaxial laminae are affected by the matrix to a larger degree than the longitudinal tensile strength and the matrix degradation due to an elevated temperature precedes that of the fibers, the former strengths degradation will be more pronounced than the reduction of the longitudinal tensile strength. This assumption is verified on the example of a SiC/Ti-6Al-4V composite. It is demonstrated that a difference in the effect of temperature on the rate of reduction of the longitudinal tensile strength versus the reduction of longitudinal compressive strength, transverse and shear strengths remains limited at moderate temperatures but increases as temperature approaches the matrix melting value. Considering particulate composites, we analyze both Ti-6Al-4V and polymeric matrix materials. The strength of particulate materials considered in the paper at elevated temperatures is mostly dictated by the strength of the matrix that is highly sensitive to thermal environments.

ARTICLE HISTORY
Received 20 December 2024
Accepted 24 February 2025

KEYWORDS
Composite lamina; composite materials; particulate composites; strength; temperature effects

1. Introduction

Temperature affects the properties of all materials found in nature. However, its effect on the mechanical response of structures is sometimes disregarded in the analysis. In numerous relatively recent studies this shortcoming has been addressed and a large number of papers include the effect of temperature on the properties of materials, e.g., [1–18]. For a brief review of these papers, see [19]. These studies considered isotropic and composite materials and addressed numerous aspects of the analysis, including strength, stiffness, dynamic problems, and micromechanics.

Experimental, analytical, and numerical studies demonstrated that the strength of composites decreases at elevated temperatures. An example of such investigations is the study of the flexural strength of carbon fiber reinforced polymers in three-point bending tests in the range of temperature from $-100\,^{\circ}\mathrm{C}$ to $100\,^{\circ}\mathrm{C}$ [20]. A finite element study of the transverse strength of composites at elevated temperatures included the coating of the fibers in the analysis and demonstrated that the strength decreases at elevated temperatures due to the failure of the coating/matrix interface

CONTACT Victor Birman vbirman@mst.edu Professor Emeritus of Mechanical Engineering, Missouri University of Science and Technology, Rolla, Missouri 65409, USA.

and the matrix [21]. However, the effect of temperature on the material properties was not considered in this investigation. Experimental research considering the effect of temperature on the strength and fatigue of silicon fiber, Ti-24Al-11Nb matrix composites in comparison to typical aerospace nickel-based superalloy, titanium alloy and titanium-aluminum alloy was undertaken in [22]. While unidirectional SiC-aluminum composites had a clear advantage over metallic counterparts, composite laminates did not possess such benefits reflecting a need in a skillful tailoring of laminated structures. The detrimental effect of the content of oxygen in the matrix of SiC-fiber, titanium matrix alloy on the high-temperature tensile strength was investigated in [23]. A study on the effect of several parameters on the longitudinal tensile strength of short-fiber polymeric matrix composites at elevated temperatures was undertaken in [24]. The analytical solution presented in this paper accounted for residual thermal stresses, probabilistic fiber length Weibull distribution, and fiber orientation. Transverse tensile strength of SiC fiber, Ti-6Al-4V composites at elevated temperatures was studied by FEA in [25] where it was demonstrated that while residual stresses affect the stress corresponding to the onset of fiber-matrix debonding, the collapse stress was little influenced by these stresses.

In this paper, we analyze the effect of temperature on the strength of a unidirectional composite lamina and on the strength of particulate composites. In the former composites, we concentrate on the comparison of thermal effects on five different strengths, including longitudinal and transverse tensile and compressive strengths, and the shear strength in the planes parallel to the fibers. In particulate composites, we analyze longitudinal tensile strength.

Numerical examples are presented for SiC fiber, Ti-6Al-4V metal matrix laminae since metal matrix composites are extensively used in high-temperature applications. Particulate composites considered in this paper had both metallic (Ti-6Al-4V) and four different polymeric matrices.

It is demonstrated in the paper that an elevated temperature results in a large reduction in matrix-dominated strengths, i.e., the strength under longitudinal compression, transverse tensile and compressive and in-plane shear loadings. The longitudinal tensile strength dominated by fibers is reduced to a comparable degree in the range of considered temperatures. However, the matrix-dominated strength degradation becomes more prominent as the temperature approaches the melting point of the matrix, while the longitudinal strength remains relatively high because of the residual strength of the fibers.

In particulate materials, the tensile strength is compromised by the failure of the particle-matrix interface and the subsequent cracking of the matrix. Thus, the properties of the matrix have a dominant effect determining the strength. It is demonstrated that a higher filler (particle) volume fraction results in a reduction of the strength in the entire range of temperatures as a result of the stress concentration around the particles. The strength decreases with temperature in all five particulate materials considered in the example.

Reflecting the numerical results, it is emphasized that strict control should be used in the manufacturing process of all composites. Such control is particularly important for fiber-reinforced materials subjected to compression during a lifetime where fiber misalignment can dramatically reduce the strength in the entire range of operating temperatures.

2. Analysis

2.1. Longitudinal, transverse, and in-plane shear strength-temperature relationships

2.1.1. Longitudinal tensile strength

The analysis of the longitudinal tensile strength has been presented in a number of papers, such as [24,26–31]. A comprehensive comparison between various methods is outside the scope of this paper, instead we concentrate on several approaches to the problem and compare the results to check whether that they are in good agreement and predict the effect of temperature on the strength.

The first method considered in this paper was presented in the book [32]. Extrapolating this approach to account for the effect of temperature, one has to compare the ultimate tensile strains of the fibers and matrix:

$$\varepsilon_f^u(T) = \frac{s_f^u(T)}{E_f(T)}, \quad \varepsilon_m^u(T) = \frac{s_m^u(T)}{E_m(T)} \tag{1}$$

where $s_f^u(T)$ and $s_m^u(T)$ are the ultimate tensile strengths of the fiber and matrix, and $E_f(T)$ and $E_m(T)$ are their moduli of elasticity, respectively. Note that Eq. (1) are written by the assumption that both the fiber and matrix are linearly elastic materials up to the ultimate tensile failure.

If the fiber fails first, the longitudinal tensile strength in the composite is obtained by

$$s_L^{(+)}(T) = s_f^u(T)\left(V_f + V_m\frac{E_m(T)}{E_f(T)}\right) \tag{2}$$

where V_f and V_m are the volume fractions of the fibers and matrix, respectively.

On the other hand, if the matrix fails prior to the fibers, the ultimate tensile strength is

$$s_L^{(+)}(T) = s_m^u(T)\left(V_m + V_f\frac{E_f(T)}{E_m(T)}\right) \tag{3}$$

It should be noted that Eqs. (2) and (3) disregard statistical aspects of the strength distribution in the fibers and matrix. These equations associate the ultimate longitudinal failure with a somewhat simplified model where all fibers fail simultaneously neglecting stress transfer from broken to intact fibers. In the case where the fibers break prior to the matrix, the interfacial shear stress and the shear lag problem have to be analyzed to better assess the ultimate strength (e.g., [33]).

The Weibull distribution [34] of the fiber strength was assumed in [35] that presented a closed form formula for the strength of the composite material:

$$s_L^{(+)}(T) = V_f\left[\frac{16\tau_{pm}^2(T)L_0\sigma_{f0}^{\rho}(T)}{(\rho+2)d_f^2}\right]^{\frac{1}{\rho+2}} e^{-\frac{1}{\rho+2}} \tag{4}$$

where the matrix is assumed elastic perfectly plastic with the shear yield strength $\tau_{pm}(T)$, ρ is the Weibull modulus, L_0 is the gauge length, d_f is the fiber diameter, and $\sigma_{f0}(T)$ is the characteristic fiber strength measured at the gauge length. The results generated using this equations were in a good agreement with experimental data for carbon/epoxy composites. However, since the materials considered in this study were polymeric matrix composites, we cannot use it in the numerical analysis below concentrating on a metal-matrix material.

Extensive studies of the ultimate longitudinal tensile strength of unidirectionally oriented fiber-reinforced polymeric, metal-matrix, and ceramic composites were conducted by Curtin and his associates [31,36,37] employing the Weibull distribution of the fiber strength. In particular, a closed form expression for the ultimate tensile strength was obtained in [37]

$$s_L^{(+)}(T) = V_f\sigma_{f0}(T)\left(\frac{\rho}{2}\right)^{\frac{\rho}{\rho+1}}\left(1 - e^{-\frac{2}{\rho}}\right) + V_m\sigma_y(T) \tag{5}$$

As was shown in [37], at $\rho = 10$, the model predictions for a notch strength of Ti-1100 matrix, SCS-6 SiC fiber composites were in close agreement with the Batdorf model [38]. The discrepancy with the experimental results was small. Thus, this value of the Weibull modulus was adopted in the subsequent calculations.

The characteristic fiber strength proportional to the critical fiber bundle stress at the gauge length L_0 in the above equation is

$$\sigma_{f0}(T) = \left(\sigma_f^{\rho}(T)\frac{\tau(T)L_0}{r_f}\right)^{\frac{1}{\rho+1}} \tag{6}$$

where $\sigma_f(T)$ is the stress carried by a bundle of fibers, r_f is the fiber radius, $\tau(T)$ is the interfacial sliding resistance. In [36], for Nicalon/CAS composites, $r_f = 7.5\ \mu m, \tau(T) = 20\ MPa$.

It was also shown in [37] that the results obtained by the modified rule of mixtures were in reasonably good agreement with those generated by the alternative theories predicting the ultimate longitudinal tensile stress that was within 10% of those available from other theories and overestimating the experimental results by about 20%. The above-mentioned modified rule of mixtures is

$$s_L^{(+)}(T) = V_f\sigma_{f0}(\mathrm{T}) + V_m\sigma_y(T) \tag{7}$$

However, the results generated by the modified rule of mixtures were larger than those obtained by Eq. (5) that yielded the predictions that were closer to the experimental data.

Finally, a very simple formula for the estimation of the tensile longitudinal strength was suggested in https://www.doitpoms.ac.uk/tlplib/fibre_composites/strength.php for the case where the matrix ultimate strength is much lower than that of the fibers so that the strength of the composite is determined by the strength of the fibers. In this case, disregarding the probabilistic distribution of the strength of the fibers, the ultimate strength of the composite is

$$s_L^{(+)}(T) = V_f s_f^u(T) \tag{8}$$

Note that this equation may be quite useful for the estimate of the strength of composites operating close to the melting temperature of the matrix where the contribution of the latter to the strength becomes negligible. Furthermore, this equation can be modified by characterizing the strength of the fibers as a probabilistic quantity.

2.1.2. Longitudinal compressive strength and in-plane shear strength

In this paper, we consider composites with brittle fibers. Accordingly, the principal mode of failure is kinking. The compressive composite stress resulting in kinking was evaluated by Budiansky [39], and further discussed in [40]. These results are extrapolated here to emphasize that the properties are temperature dependent:

$$s_L^{(-)}(T) = \frac{G(T)}{1 + {}^{\phi G(T)}\big/_{\tau_y(T)}} \tag{9}$$

where $G(T)$ is the shear modulus of the composite, ϕ is the maximum initial misalignment angle of the kink in radians, and $\tau_y(T)$ is the shear yield stress of the composite material. If the misalignment is absent and the kink is normal to the load direction, $\phi = 0$ and the formula converges to the result suggested by Rosen [41]. On the other hand, if the misalignment is large, ${}^{\phi G_m(T)}\big/_{\tau_y(T)} \gg 1$ and the formula for the compressive strength is reduced to the result suggested by Argon [42]. In numerical examples in this paper, we consider a band of longitudinal compressive strength with the angle of fiber misalignment varying from 0 to 5°.

The shear yield stress of the composite can be determined using the matrix shear strength divided by the shear stress concentration factor [32]:

$$\tau_y(T) = \frac{\tau_m^{shear}(T)}{k_\tau(T)} \tag{10}$$

where

$$k_\tau(T) = \frac{1 - V_f\left(1 - {G_m(T)}\Big/{G_f(T)}\right)}{1 - \sqrt{\frac{4V_f}{\pi}}\left(1 - {G_m(T)}\Big/{G_f(T)}\right)} \tag{11}$$

The shear modulus of the composite can be obtained by one of the numerous micromechanical methods. In particular, the Halpin-Tsai method [43] that was shown to be quite accurate [44] yields

$$\frac{G(T)}{G_m(T)} = \frac{1 + \eta(T)V_f}{1 - \eta(T)V_f} \tag{12}$$

where

$$\eta(T) = \frac{{G_f(T)}\Big/{G_m(T)} - 1}{{G_f(T)}\Big/{G_m(T)} + 1} \tag{13}$$

Among other studies relevant to the longitudinal compressive strength is a comparison of the methods used to predict the compressive strength of fiber-reinforced composites [45] that experimentally demonstrated the advantage of the Budiansky-Fleck model, i.e., Eq. (9).

Note that the solution presented above does not include the probabilistic aspect that can influence the prediction of the strength. This is a probabilistic distribution of the initial fiber misalignment. Mentioned here is a comprehensive review of probabilistic models employed in the analysis of the strength of polymeric matrix composites [46]. The probabilistic strength problem, i.e., the effect of a random fiber misalignment, was considered in [47] using experimental measurements conducted on a carbon/epoxy material to determine a power spectral density function used to evaluate the misalignment and the Monte Carlo method to specify the strength. Due to the lack of data for the metal matrix composite considered in numerical examples, this solution is not discussed here.

2.1.3. Transverse tensile strength

One of the models evaluating this strength is based on the evaluation of the stress concentration or strain concentration factor in the isotropic matrix adjacent to the fiber-matrix interface [32]. According to the approach utilizing the maximum stress failure criterion,

$$s_T^{(+)}(T) = \frac{1}{k_\sigma(T)}\left[s_m^u(T) - \sigma_{rm}(T)\right] \tag{14}$$

where σ_{rm} is a residual stress in the matrix.

The result based on the maximum strain failure criterion is

$$s_T^{(+)}(T) = \frac{1 - \nu_m(T)}{k_\sigma(T)[(1 + \nu_m(T))(1 - 2\nu_m(T))]}\left[s_m^u(T) - \varepsilon_{rm}(T)E_m(T)\right] \tag{15}$$

The stress concentration factor in these equations is

$$k_\sigma(T) = \frac{1 - V_f\left(1 - \frac{E_m(T)}{E_f(T)}\right)}{1 - \sqrt{\frac{4V_f}{\pi}}\left(1 - \frac{E_m(T)}{E_f(T)}\right)} \tag{16}$$

The other approach based on the elasticity solution was presented in the recent paper [48]. According to the analysis in this paper, the transverse tensile strength of the material undergoing a uniaxial transverse tension can be calculated as

$$s_T^{(+)}(T) = \frac{1}{(1+\nu_m(T))(1-2\beta(T))\left(1-5.8\gamma(T)V_f^3\right)}\sigma_y(T) \tag{17}$$

where

$$\beta(T) = \frac{G_m(T) - G_f(T)}{G_m(T) + G_f(T)(3-4\nu_m(T))}$$

$$\alpha(T) = \frac{G_m(T)\left(3-4\nu_f(T)\right) - G_f(T)(3-4\nu_m(T))}{G_f(T) + G_m(T)\left(3-4\nu_f(T)\right)}$$

$$\gamma(T) = \frac{\alpha(T) - \beta(T)}{(1-\beta(T)) - \beta(T)(1-\alpha(T))} \tag{18}$$

In Eqs. (17) and (18) the fiber is assumed isotropic, and $\nu_f(T)$ and $\nu_m(T)$ are the Poisson ratios of the fiber and matrix, respectively.

Finally, it is worth noting that a simple expression for the transverse strength was found in a good agreement with experimental data in https://www.doitpoms.ac.uk/tlplib/fibre_composites/strength.php:

$$s_T^{(+)}(T) = s_m^u(T)\left[1 - 2\sqrt{\frac{V_f}{\pi}}\right] \tag{19}$$

As is evident from Eqs. (15), (17), and (19), at the matrix melting temperature the transverse tensile strength drops to zero (residual stresses and strains are equal to zero at the melting temperature). Physically, this reflects an observation that composite laminae cannot transfer transverse loads in the absence of the matrix.

2.1.4. Transverse compressive strength

In the paper [48] transverse compressive strength was obtained as

$$s_T^{(-)}(T) = \frac{s_i(T)}{\sqrt{g_i(T)}}\left(\frac{2}{1-\beta(T)}\right) \tag{20}$$

where

$$g_i(T) = -7.71\left(0.14+\beta(T)\right)V_f^3 + 6.63\left(0.01+\beta(T)\right)V_f^2 + 0.16\left(3.00+\beta(T)\right)V_f - 0.76\left(-0.24+\beta(T)\right) \tag{21}$$

In Eqs. (20), $s_i(T)$ is the strength of the fiber-matrix interface and $\beta(T)$ is defined in Eq. (18). At the matrix melting temperature, $s_i(T) = 0$ and the composite strength is reduced to zero.

2.1.5. Tensile strength of particulate composites

A simple formula based on a comparison with experimental data was suggested in [49]. Modifying this formula to account for the effect of temperature we obtain:

$$\sigma_c^{(+)}(T) = s_m^u(T)\left(1 - 1.21V_f^{2/3}\right) \tag{22}$$

where V_f is the filler (particle) volume faction.

This prediction was found in excellent agreement with experimental data for six particulate composite materials: resin matrix with voids, SAN matrix (styrene acrylonitrile) filled with carbon particles, PPO (polyphenylene oxide) matrix with glass particles, glass/epoxy, SAN (styrene acrylonitrile resin) matrix with glass particles, and ABS (acrylonitrile butadiene styrene) matrix with glass particles. All particles considered in this paper were spherical. Note that as follows from Eq. (22) the strength of a composite with spherical inclusions cannot exceed that of the pristine matrix.

Note that Eq. (22) is derived without taking into consideration the properties of spherical inclusions. The reason is that the filler particles are assumed detached from the matrix at the breaking strain, i.e., this equation analyzes the matrix material with holes, without accounting for the contribution of the filler at the composite breaking strain.

A simple formula for the strength of a particulate composite material accounting for the filler-matrix adhesion was suggested in [50]:

$$\sigma_c^{(+)}(T) = s_m^u(T)\frac{E_c(T)}{E_m(T)}\left(1 - V_f^{1/3}\right) \tag{23}$$

However, as was demonstrated in [51], this formula does not predict the strength of polymeric composites available from experiments. A different formula, based on fitting of the predicted and experimental strength values was proposed in [51]:

$$\sigma_c^{(+)}(T) = s_m^u(T)\frac{1 - V_f}{a + bV_f + cV_f^2} \tag{24}$$

where a, b and c are fitting coefficients.

The problem with using Eq. (24) is that the fitting coefficients are specified for each particular material, i.e., this equation is not universal. For example, an excellent agreement was achieved for polyester resin matrix and $CaCO_3$ particles composites using $a = 1.00$, $b = 2.20$, $c = -5.41$, while for vinylester/$CaCO_3$ materials, the agreement between experimental strength and the strength predicted by Eq. (24) was obtained using $a = 1.00$, $b = 0.38$, $c = -1.90$. However, for each different material we have to generate a new set of experimental data to specify the fitting coefficients.

Accordingly, we employ Eq. (22) in the analysis since it has been successfully experimentally verified on six composite materials.

2.2. Properties of representative materials considered in numerical examples

The fiber-reinforced composite material selected for the numerical analysis consist of a titanium alloy matrix (Ti-6Al-4V) and silicon carbide fibers (SiC). The temperature-dependent relationships between the moduli of elasticity and the Poisson ratio of the titanium alloy and silicon carbide (SiC) are [52]:

$$\text{Titanium }(\text{Ti} - 6\text{Al} - 4\text{V}) : E_m = 122.7 - 0.056T \ (GPa) \ \nu_m = 0.289 + 32 * 10^{-6}T \tag{25}$$

$$\text{Silicon carbide }(\text{SiC}) : E_f = 416.3 - 0.021T \ (GPa) \ \nu_f = 0.171 - 3.044 * 10^{-6}T \tag{26}$$

In these equations, temperature is measured in degrees K. The modulus of elasticity of the titanium alloy calculated by Eq. (25) is equal to zero if $T = 2172$ K. This corresponds to temperature 1899 °C, while the reported melting range of this material is within 1538 °C–1649 °C (Technical Data Sheet, https://www.atimaterials.com/). This reflects a nonlinear relationship between the modulus of elasticity of Ti-6Al-4V and temperature when the latter approaches the melting point. In the absence of such a relationship for the matrix material, we present the relevant examples below for temperature increasing from the room temperature to an operational value that is well below the melting point of Ti-6Al-4V.

The ultimate tensile strength of Ti-6Al-4V depends on temperature as reflected in Technical Datasheet of Carpenter Technology "Titanium Alloy Ti 6Al-4V". The relationship between the strength and temperature up to 350 °C is almost linear and it is approximated as

$$s_m^u(T) = 936.8 - 0.642T \tag{27}$$

where the strength is measured in MPa, and the temperature is in degrees Celsius. In numerical examples this relationship is extrapolated to 500 °C.

The matrix yield stress is smaller than the ultimate tensile strength since Ti-6Al-4V demonstrates a noticeable strain hardening. Thus, we use an approximate formula based on the analysis [53]:

$$\sigma_y(T) = 800 - 0.5T \tag{28}$$

where the strength is measured in MPa, and temperature is in degrees Celsius.

The tensile strength of SiC fibers as a function of temperature does not change much in the temperature range suitable for SiC/titanium matrix composites. In the study [54] the tensile strength of Nicalon fibers was found as a function of temperature and time of exposure defined by the Larson-Miller parameter

$$\mathrm{q} = \mathrm{T}\,[\log \mathrm{t} + 22] \tag{29}$$

where t is time of exposure in hours, and T is temperature in degrees Kelvin. Assuming the time of exposure equal to one hour and temperature varying between 20 °C and 400 °C, we obtain a linear relationship:

$$s_f^u(T) = 3,016 - 0.79T \tag{30}$$

In Eq. (30), the strength is in MPa, and temperature is measured in degrees Celsius. Shear strength of Ti-6Al-4V is available from [55]. Using the data presented in this paper for the rate of loading equal to $1.8*10^3$ 1/s and extrapolating it as a linear function of temperature in the range from 25 °C to 300 °C, we obtain

$$\tau_m^{shear}(T) = 427.26 - 0.16T \tag{31}$$

where the stress is in MPa, and temperature is in degrees Celsius. This relationship has been extrapolated to 500 °C in the following analysis.

The data of the effect of temperature on the interfacial strength is adopted from [56] and [57] where it was demonstrated that the strength of the interface between a SiC fiber and Ti 6Al-4V matrix is a linear function of temperature. The interfacial shear stress is represented by

$$s_i^{shear}(T) = 150 - 0.175T \tag{32}$$

where the stress is measured in MPa, and temperature is measured in degrees Celsius. The radial yield stress $s_i(T)$ is obtained by doubling the value calculated by Eq. (32) following the recommendation in [56].

Following the results in [37], the Weibull parameter ρ =10 was adopted in computations. Characteristic fiber strength in Eqs. (5) and (7) is replaced with an experimental value available from Eq. (30).

Matrix materials considered in the analysis of the effect of temperature on the strength of particulate composites include Ti-6Al-4V, two polymeric adhesive materials, and polyester and vinylester resins. Adhesive materials represent an interest since their properties could be improved by adding nanoparticles.

The ultimate strength of epoxy adhesive XN1244 was found representing experimental data by a quadratic equation [58]:

$$s_m^u(T) = 66.522 + 0.160T - 0.00373T^2(MPa) \tag{33}$$

Eq. (33) is generated to approximate experimental strength values in the range from the room temperature to 150 °C. At higher temperatures, the strength of XN1244 sharply drops, so this temperature is unlikely to be exceeded in practical applications.

The thermal properties of the second adhesive epoxy considered in this paper are adopted from [59]. According to experimental data in this paper, the strength versus temperature relationship can be represented by a bilinear law. At a relatively slow loading rate, this law can be approximated by

$$T = 20^0C - 40^0C\text{: } s_m^u(T) = 66.87 - 0.530T(MPa)$$
$$T = 40^0C - 60^0C\text{: } s_m^u(T) = 71.59 - 0.652T(MPa) \tag{34}$$

The relationship between the tensile strength and temperature of polyester resin in the range from 20 °C to 60 °C found in [60] was nonlinear. This relationship can be approximated by a quadratic function

$$s_m^u(T) = 31.000 + 0.625T - 0.01625T^2(MPa) \tag{35}$$

The tensile strength of a vinylester resin was experimentally measured as a function of temperature in [61,62]. In this paper, we use the measurements in [62] at a very slow loading strain rate of 0.0001 (1/s) (data used is taken from Table 1 of this reference) approximating it by a quadratic equation:

$$s_m^u(T) = 97.3 - 0.548T - 0.00123T^2(MPa) \tag{36}$$

3. Numerical examples

Longitudinal tensile strengths of SiC/Ti-6Al-4V composites are shown as functions of temperature in Figures 1 ($V_f = 0.2$) and 2 ($V_f = 0.5$). All theories compared in these figures predict an identical trend, i.e., a reduction of the strength with a higher temperature. Remarkably, the results obtained by Eqs. (2) or (3) and Eq. (7) were in a close agreement. This could be expected since these equations represent various interpretations of the rule of mixtures for composites with a uniform fiber strength. However, the results obtained by Eq. (5) were more conservative as could be anticipated since they account for the Weibull distribution of the fiber strength. The results

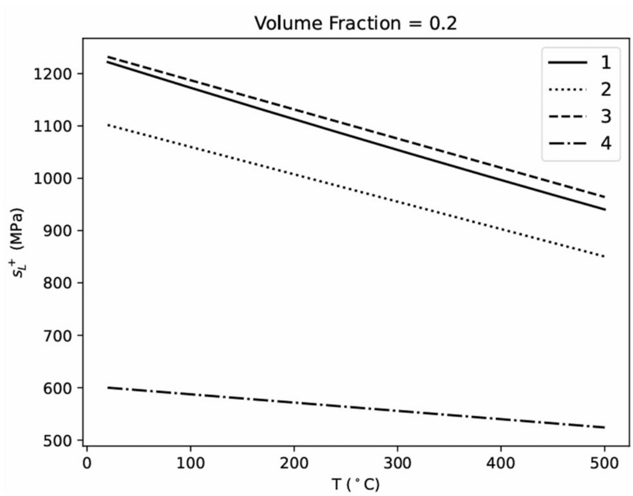

Figure 1. Longitudinal tensile strength of SiC/Ti-6Al-4V composites. Fiber volume fraction is $V_f = 0.2$. Curve 1 is obtained by Eqs. (2) and (3). Curve 2 is obtained by Eq. (5). Curve 3 is obtained by Eq. (7). Curve 4 is obtained by Eq. (8).

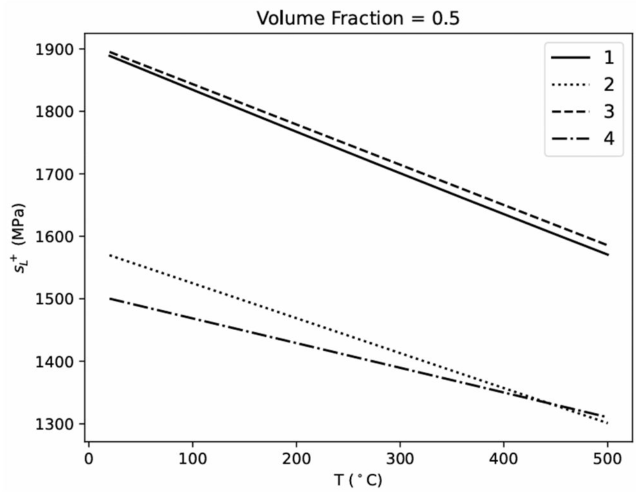

Figure 2. Longitudinal tensile strength of SiC/Ti-6Al-4V composites. Fiber volume fraction is $V_f = 0.5$. Curve 1 is obtained by Eqs. (2) and (3). Curve 2 is obtained by Eq. (5). Curve 3 is obtained by Eq. (7). Curve 4 is obtained by Eq. (8).

obtained by Eq. (8) are most conservative, but they are probably inaccurate since both the contribution of the matrix outside of the vicinity to the matrix melting temperature as well as the probabilistic distribution of the strength of the fibers are neglected. However, a modification of this equation could be adopted in the vicinity to the matrix melting temperature accounting for the probabilistic fiber strength distribution. Similar to the observation in [37], the modified rule of mixtures (Eq. (7)) predicted a higher strength than Eq. (5). A larger fiber volume fraction results in a higher strength as could be expected considering that the fibers carry the major share of the longitudinal tensile load. A reduction of the strength in the range of temperature from 0° to 500 °C predicted by Eq. (5) is in the range from 18% to 23%.

Longitudinal compressive strengths of SiC/Ti-6Al-4V composites are presented in Figures 3 and 4 for two different fiber volume fractions as functions of temperature and the angle of misalignment of the fibers. While the strength decreases with an elevated temperature for all considered fiber orientation misalignments, from 0° to 5°, there is an abrupt drop in the strength in the range from 0° to 3°. The effect of an even larger misalignment, i.e., the difference between the cases of 3° and 5° is relatively smaller. The phenomenon is demonstrated in the inserts in Figures 3 and 4 evaluated at 0 °C, 100 °C and 500 °C. A similarly abrupt reduction in the strength as a result of fiber misalignment was also previously reported for carbon/epoxy in [32]. An important practical conclusion from Figures 3 and 4 is that control of the manufacturing process is vitally important for composites subjected to compression during lifetime since even a small fiber misalignment can drastically reduce the strength. Furthermore, a misalignment of fibers should be treated as a probabilistic phenomenon, and a probabilistic model predicting the longitudinal compressive strength of composites might be preferable to deterministic counterparts. Note that a reduction in the strength in the investigated range of temperature was about 27% and 19% for $V_f = 0.2$ and 0.5, respectively, for perfectly aligned fibers, i.e., this reduction is close to the reduction observed in the case of longitudinal tensile strength.

The shear yield strength of the composite is shown in Figure 5 for two fiber volume fractions. As can be observed, this strength is actually higher in the case of a smaller fiber volume fraction. The reason is an increasing shear stress concentration factor in the case of a larger fiber volume fraction. The reductions in the shear yield strength as temperature increases from 0 °C to 500 °C are about 23% for both fiber volume fractions.

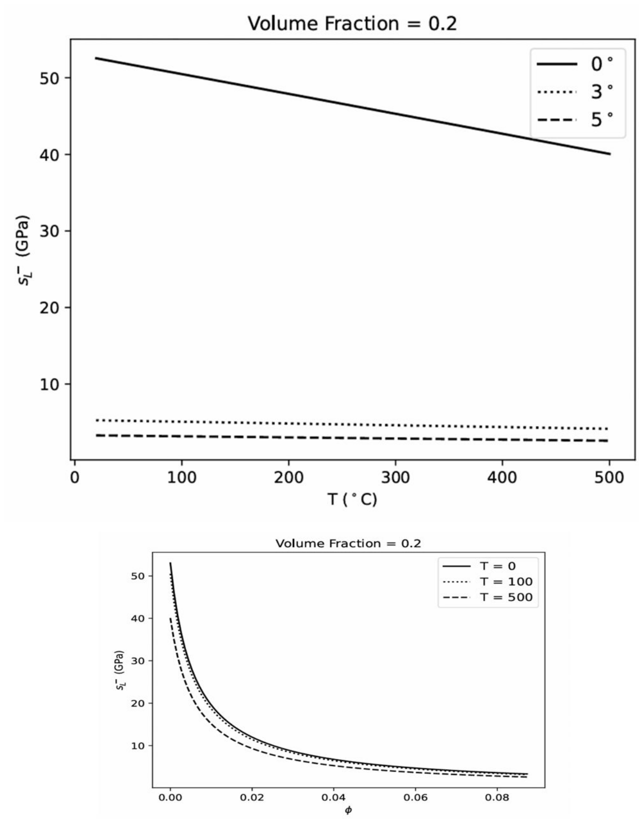

Figure 3. Longitudinal compressive strength of SiC/Ti-6Al-4V composites. Fiber volume fraction is $V_f = 0.2$. The fiber misalignment angle is equal to 0°, 3°, and 5°. The lower figure demonstrates the change in the strength as a function of the angle of misalignment at three different temperatures.

Transverse tensile strengths of composites are shown as functions of temperature in Figures 6 and 7. The scatter between the predictions obtained by various methods is evident. However, all theories predict a very significant drop of the strength as a result of an elevated temperature. The strength is a little higher at a smaller fiber volume fraction (Figure 6). The physical reason is that transverse strength is mostly dictated by the matrix and at a smaller fiber volume fraction there are fewer vulnerable regions of stress concentration at the fiber-matrix interface where fracture originates. Also, the stress concentration factor is higher in the composite with a larger fiber volume fraction, similar to the case of the in-plane shear. In spite of a large mismatch between the theories, the strength decreases linearly with temperature according to all considered methods. Note that the reduction in the strength due to temperature increasing from 0 °C to 500 °C is larger than in the case of the longitudinal tensile strength varying between 25% and 40%, dependent on the theory used for the calculation and the fiber volume fraction. This reflects on the mechanism of the stress transfer: while longitudinal tensile stresses are mostly transferred by the fibers, transverse stresses are transferred through the matrix that is affected by temperature more than the fibers.

Transverse compressive strength is displayed in Figure 8. It is interesting to note that while a higher fiber volume faction caused a reduction in the transverse tensile strength, the trend observed in Figure 8 is opposite. This reflects the observation that while fracture originating from the fiber-matrix interface caused the loss of strength in the former case, it does not occur under compression. Instead, the loss of strength is probably due to crushing of the matrix. Out of all strengths considered here the reduction of transverse compressive strength with temperature was

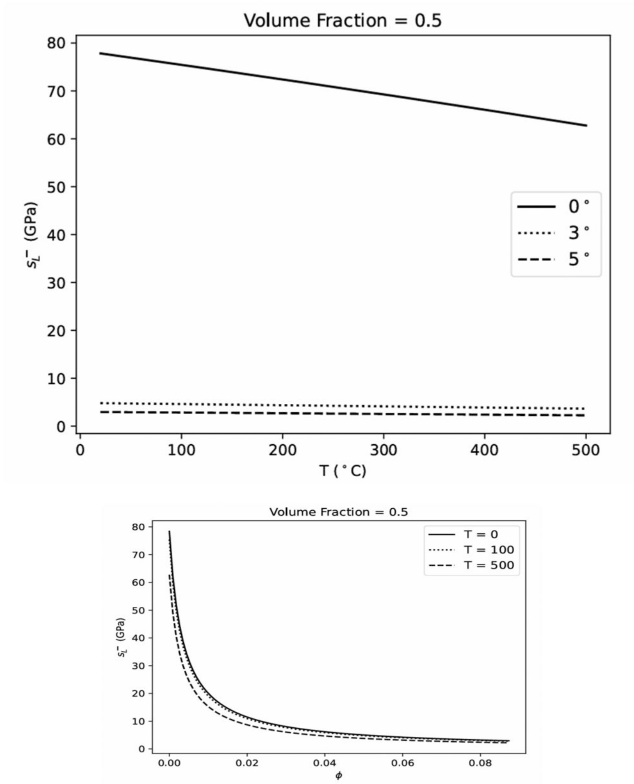

Figure 4. Longitudinal compressive strength of SiC/Ti-6Al-4V composites. Fiber volume fraction is $V_f = 0.5$. The fiber misalignment angle is equal to 0°, 3°, and 5°. The lower figure demonstrates the change in the strength as a function of the angle of misalignment at three different temperatures.

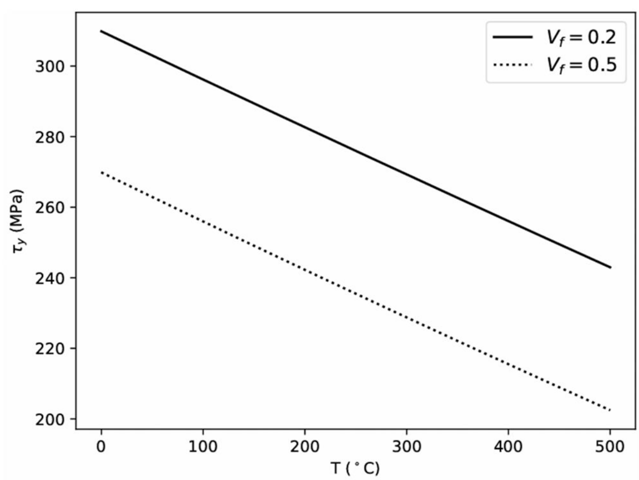

Figure 5. Shear yield strength of SiC/Ti-6Al-4V composites with fiber volume fractions equal to $V_f = 0.2$ and $V_f = 0.5$.

the most prominent (about 63% for $V_f = 0.2$ and 59% for $V_f = 0.5$). Note that the transverse compressive strength of SiC fiber, titanium matrix composites is much higher than their tensile strength. This has been confirmed in the previous experiments (e.g., [63]).

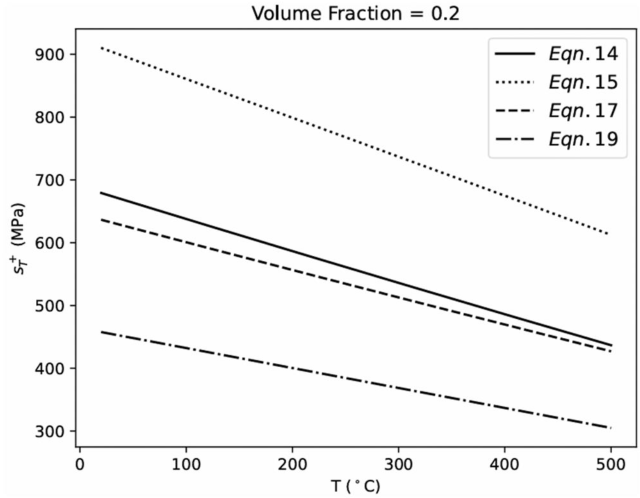

Figure 6. Transverse tensile strength of SiC/Ti-6Al-4V composites. Fiber volume fraction is $V_f = 0.2$.

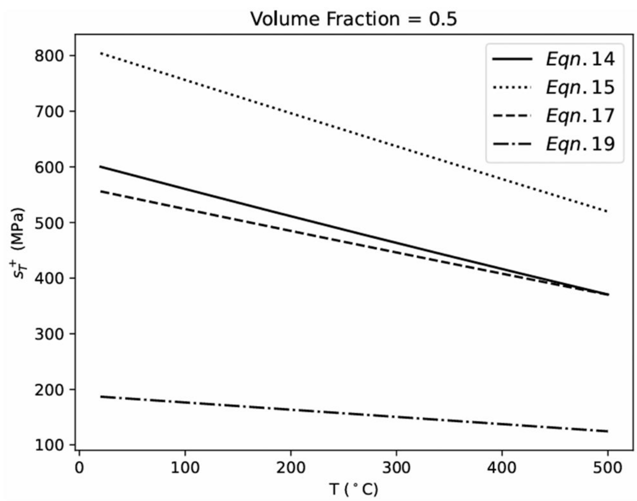

Figure 7. Transverse tensile strength of SiC/Ti-6Al-4V composites. Fiber volume fraction is $V_f = 0.5$.

The comparison of a relative loss of strength in five different cases considered above indicates that transverse strength decreases with temperature at a higher rate than the longitudinal and shear strengths. This is due to a temperature-induced degradation of the matrix. Rather surprisingly, a reduction of the shear strength is of the same order as that of the longitudinal tensile strength. The situation drastically changes as temperature approaches the matrix melting value and the only remaining strength is the fiber-dominated longitudinal tensile strength as is illustrated below.

Tensile strengths of several particulate composites as functions of temperature and volume fraction of the particles are depicted in Figures 9–13. While the volume fractions of silicon particles embedded in Ti-6Al-4V matrix are chosen equal to 0.2 and 0.5, (Figure 9) and 0.3 and 0.5 in polymeric particulate composites (Figures 12 and 13), in epoxy adhesives particle volume fractions are equal to 0.1 and 0.2 (Figures 10 and 11). This is because high volume fractions of inclusions embedded in epoxy adhesives are unlikely.

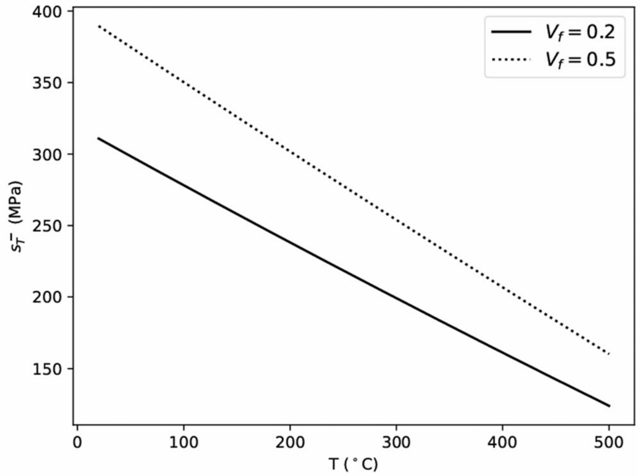

Figure 8. Transverse compressive strength of SiC/Ti-6Al-4V composites. Fiber volume fractions are $V_f = 0.2$ and $V_f = 0.5$.

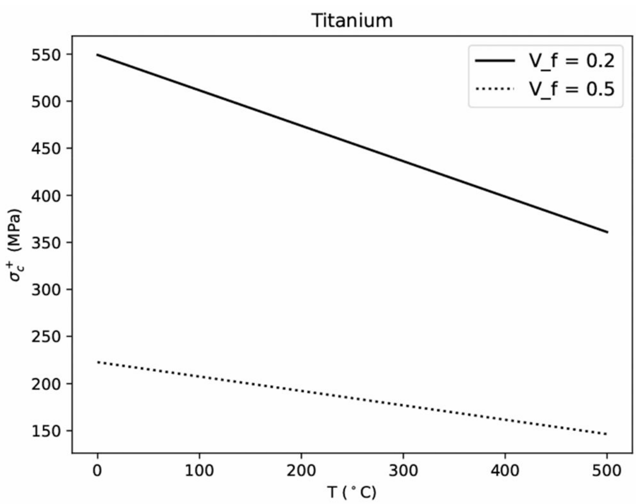

Figure 9. Tensile strength of particulate SiC/Ti-6Al-4V composites. The filler (particle) volume fractions are $V_f = 0.2$ and $V_f = 0.5$. Particle-to-matrix adhesion is neglected.

In all cases demonstrated in Figures 9–11 and 13 a higher particle volume fraction resulted in a reduced tensile composite strength. This is the result of stress concentrations in the matrix along the particle-matrix interface. The situation is different in the case of polyester matrix with embedded $CaCo_3$ particles (Figure 12) where particles increase the strength at temperatures over 45 °C. The reason for the different behavior of these composites should probably be considered at the micromechanical level analyzing local stresses at the particle-matrix interface and fracture propagation in the vicinity to this interface.

It is remarkable that some of the results demonstrated above were generated using linear relationships between the properties and temperature for inclusions and matrix. For example, for SiC/Ti-6Al-4V composites, the moduli of elasticity and the Poisson ratios of the fibers and matrix are given by Eqs. (25) and (26), the tensile strength of the matrix is determined by Eqs. (27) and (28), while its shear strength is determined by Eq. (31), and the ultimate tensile strength of the fibers is provided by Eq. (30). All these equations are linear. However, as is discussed below, the melting temperature of Ti-6Al-4V is smaller than the value that results in a reduction of its

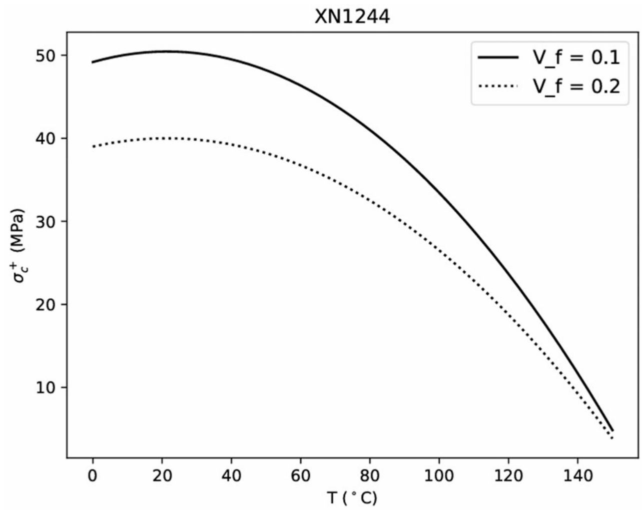

Figure 10. Tensile strength of particulate epoxy adhesive XN1244. The filler (particle) volume fractions are $V_f = 0.1$ and $V_f = 0.2$. Particle-to-matrix adhesion is neglected.

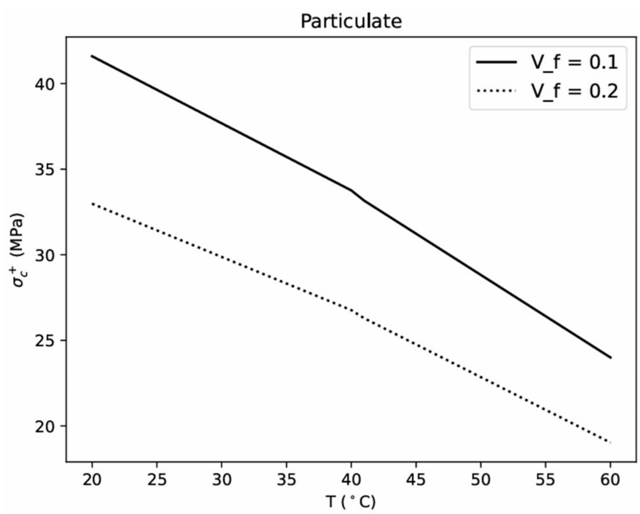

Figure 11. Tensile strength of particulate epoxy adhesive. The filler (particle) volume fractions are $V_f = 0.1$ and $V_f = 0.2$. Particle-to-matrix adhesion is neglected.

stiffness determined from Eq. (25) to zero. This implies that while the property-temperature relationships of this material remain linear in the moderate temperature range, they are nonlinear at higher temperatures. We do not have a complete information about the effect of high temperature approaching the melting value on the properties of titanium matrices and SiC fibers. Thus, the examples presented above are limited to the temperature range where the properties are linear functions of temperature.

Compare the longitudinal tensile strength to compressive longitudinal and in-plane shear strengths of SiC/Ti-6Al-4V at the matrix melting temperature, i.e., in the range of 1538 °C–1649 °C corresponding to 1811K–1922K (see discussion after Eq. (26)). In this range of temperatures, the fibers retain strength since according to Eq. (30), their strength is reduced to zero only at 3,818 °C. Therefore, even if the fiber strength-temperature relationship becomes nonlinear at high temperatures, it is apparent that the matrix fails first. Using Eq. (26) we calculate the moduli

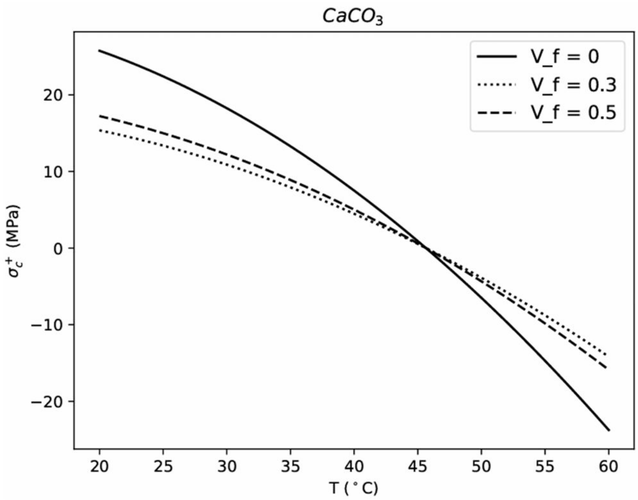

Figure 12. Tensile strength of particulate polyester resin with $CaCO_3$ particles. The filler (particle) volume fractions are $V_f = 0$, 0.3 and 0.5. Particle-to-matrix adhesion is accounted for.

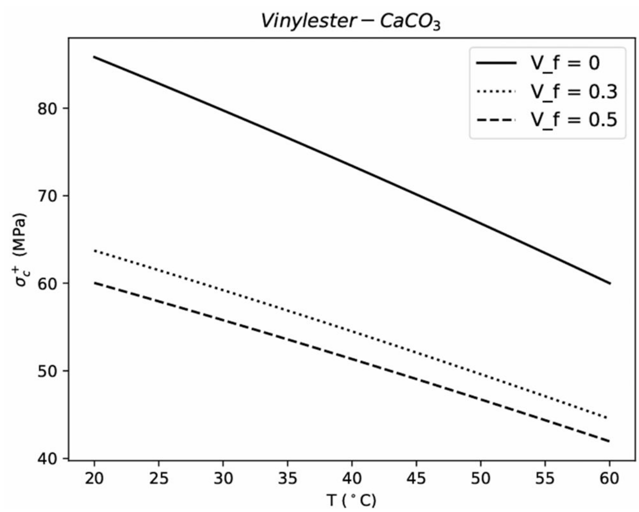

Figure 13. Tensile strength of particulate vinylester/$CaCO_3$. The filler (particle) volume fractions are $V_f = 0$, 0.3, and 0.5. Particle-to-matrix adhesion is accounted for.

of elasticity of the fibers at temperatures equal to 1811K and 1922K that are equal to 378 GPa and 376 GPa, respectively. Since the stiffness of the matrix is reduced to zero at the melting temperature, the in-plane shear strength of the composite also becomes equal to zero, according to Eq. (10). The longitudinal compressive strength is calculated by Eq. (9) that is modified by dividing the numerator and denominator by the shear modulus of the composite yielding. Then this strength at the melting temperature is equal to zero. This is a logical conclusion since even though the fibers are in theory capable of carrying the load even at the matrix melting temperature, they cannot resist compression and buckle due to their very small stiffness. Predictable, the tensile strength of particulate composites is reduced to zero at the matrix melting temperature as follows from Eqs. (22) and (23).

The situation is different when we analyze the longitudinal tensile strength since it is mostly contributed by the fibers. Since at the melting temperature the matrix does not contribute to the resistance of the load, we are justified using Eq. (8). The tensile strengths of the fibers in this equation in the temperature range from 1538 °C to 1649 °C are estimated from Eq. (30), neglecting a possible nonlinearity in the strength-temperature relationship at high temperatures. Accordingly, we calculate the values of 1801 GPa and 1713 GPa at 1538 °C to 1649 °C, respectively. The corresponding composite strength can now be calculated from Eq. (30) by multiplying these values by the fiber volume fraction.

Therefore, we can observe that the effect of temperature on the matrix-dominated strengths of composites is of the same order as this effect on the strength dominated by the fibers, i.e., the longitudinal tensile strength, in the moderate temperature range. However, at high temperatures approaching the melting temperature of the matrix the difference between two above-mentioned classes of the strength becomes evident. While the material is still capable of carrying longitudinal tensile stresses until the fibers fail, the strengths dominated by the matrix contribution are reduced to zero.

4. Conclusions

1. Effect of temperature on strengths of unidirectional fiber and particulate composites is analyzed by several available theories. Numerical results are presented for a representative metal matrix SiC fiber unidirectional composites and for several particulate composites.
2. The effect of the inclusion volume fraction is considered for both fiber-reinforced and particulate composites.
3. It is shown that although several theories yield broadly different strength predictions, all of them indicate that the strength decreases as a result of a higher temperature.
4. Longitudinal tensile strength increases in composites with a larger fiber volume fraction since the fibers carry a large share of tensile load.
5. Longitudinal compressive strength sharply decreases as a result of an even small fiber misalignment angle. A larger fiber volume fraction results in an increase in the strength since the fibers transfer a higher load than the matrix and their stiffness and strength are less affected by temperature. It is suggested that since the fiber misalignment after the processing is a random quantity there is a need in comprehensive statistical models accounting for the statistical phenomena to estimate the longitudinal compressive strength.
6. Yield shear strength is negatively affected by a larger fiber volume fraction as a result of a higher stress concentration at the fiber-matrix interface.
7. Transverse tensile strength can be estimated by a number of theories that predict significantly differing results. While the choice of the most accurate theory is outside the scope of this paper, it is observed that the drop in the transverse tensile strength as the result of an elevated temperature is larger than the corresponding drop for longitudinal strengths. This is a reflection of the mechanism of the load transfer that predominantly occurs through the matrix, rather than through the fibers. The effect of the fiber volume fraction is smaller than in the case of longitudinal tension.
8. Transverse compressive strength is affected by temperature to a larger degree than other strengths. An increase in the fiber volume fraction is beneficial for this strength.
9. Tensile strengths as functions of temperature were considered for five particulate composites. One of them was SiC/Ti-6Al-4V and four others were polymeric matrix composites, including two adhesives. In all cases, the strength decreased with temperature as could be predicted from Eqs. (22) and (23). The presence of particles (or a larger volume fraction of particles) resulted in a reduction in the strength, with the exception of $CaCO_3$ particles, the polyester matrix composite at temperatures exceeding 45 °C. Physically, a reduction in the strength occurring at a larger particle concentration can be explained by a larger number of local stress concentrations occurring at the particle-matrix interface.

10. A difference between the rate of temperature-induced decrease of fiber-dominated longitudinal tensile strength and matrix-dominated strengths (longitudinal compressive strength, transverse tensile and compressive strengths, shear strength) increases as temperature approaches the matrix melting range. At the matrix melting temperature the latter strengths drop to zero, while the lamina retains the longitudinal tensile strength.
11. It is recommended to develop and implement statistical models in the analysis of longitudinal compressive strength, possibly using a Weibull distribution of the angle of misalignment of the fibers. In particulate composites, a statistical model could also be useful reflecting a nonuniform distribution of particles throughout the material.

Acknowledgement

Discussions with Dr. Ajey Dambal are warmly appreciated.

Disclosure statement

No potential conflict of interest was reported by the author(s).

References

[1] A. G. Gibson, *et al.*, "Model for the thermal performance of thick composite laminates in hydrocarbon fires," *Rev. Inst. Fr. Pét*, vol. 50, no. 1, pp. 69–74, 1995. DOI: 10.2516/ogst:1995007.
[2] G. Q. Li, *et al.*, "Experimental studies on the properties of constructional steel at elevated temperatures," *J. Struct. Eng.*, vol. 129, no. 12, pp. 1717–1721, 2003. DOI: 10.1061/(ASCE)0733-9445(2003)129:12(1717).
[3] V. Pradeep, N. Ganesan and K. Bhaskar, "Vibration and thermal buckling of composite sandwich beams with viscoelastic core," *Comp. Struct.*, vol. 81, no. 1, pp. 60–69, 2007. DOI: 10.1016/j.compstruct.2006.05.011.
[4] M. A. Vaz, J. C. R. Cyrino and A. C. Neves, "Initial thermo-mechanical post-buckling of beams with temperature-dependent physical properties," *Int. J. Non-Linear Mech.*, vol. 45, no. 3, pp. 256–262, 2010. DOI: 10.1016/j.ijnonlinmec.2009.11.006.
[5] A. P. Mouritz, *et al.*, "Mechanical property degradation of naval composite materials," *Fire Technol.*, vol. 47, no. 4, pp. 913–939, 2011. DOI: 10.1007/s10694-009-0125-5.
[6] D. F. Cui and H. Y. Hu, "Thermal buckling and natural vibration of the beam with an axial stick-slip-stop boundary," *J. Sound Vib.*, vol. 333, no. 8, pp. 2271–2282, 2014. DOI: 10.1016/j.jsv.2013.11.042.
[7] B. Jo, W. Sagawa and K. Okamoto, "Measurement of buckling load for metallic plate columns in severe accident conditions," *Nucl. Eng. Des.*, vol. 274, pp. 118–128, 2014. DOI: 10.1016/j.nucengdes.2014.04.018.
[8] ŞD. Akba and T. Kocatürk, "Post-buckling analysis of Timoshenko beams with temperature-dependent physical properties under uniform thermal loading," *Struct. Eng. Mech.*, vol. 44, no. 1, pp. 109–125, 2012. DOI: 10.12989/sem.2012.44.1.109.
[9] W. Y. Wang, B. Liu and V. Kodur, "Effect of temperature on strength and elastic modulus of high-strength steel," *J. Mater. Civ. Eng.*, vol. 25, no. 2, pp. 174–182, 2013. DOI: 10.1061/(ASCE)MT.1943-5533.0000600.
[10] A. J. P. M. Correia and J. P. C. Rodrigues, "Fire resistance of steel columns with restrained thermal elongation," *Fire Safety J.*, vol. 50, pp. 1–11, 2012. DOI: 10.1016/j.firesaf.2011.12.010.
[11] S. Cheng, L-y Li and B. Kim, "Buckling analysis of partially protected cold-formed steel channel-section columns at elevated temperatures," *Fire Safety J.*, vol. 72, pp. 7–15, 2015. DOI: 10.1016/j.firesaf.2015.02.010.
[12] S. Uzny, Ł. Kutrowski and T. Skrzypczak, "Free vibrations of the column taking into account compressive and thermal load," *Vibr. Phys. Syst.*, vol. 30, no. 2, pp. 2019211, 2019.
[13] X. Wang, *et al.*, "The influence of temperature on the microstructure and properties of Nb-V-Ti-Mo complex microalloyed high-strength fire-resistant steel," *Metals*, vol. 11, no. 11, pp. 1670, 2021. DOI: 10.3390/met11111670.
[14] G. Q. Li and L. X. Song, "Mechanical properties of TMCP Q690 high strength structural steel at elevated temperatures," *Fire Safety J.*, vol. 116, pp. 103190, 2020. DOI: 10.1016/j.firesaf.2020.103190.
[15] S. Banerji and V. Kodur, "Effect of temperature on mechanical properties of ultra-high performance concrete," *Fire Materials*, vol. 46, no. 1, pp. 287–301, 2022. DOI: 10.1002/fam.2979.

[16] S. Lee and J. H. Kim, "Thermomechanical vibration and stability of effectively homogenized FGM beam with temperature-dependent shear correction factors," *J. Comp. Mater.*, vol. 57, no. 2, pp. 253–264, 2023. DOI: 10.1177/00219983221143490.

[17] V. Birman, "Thermal buckling and postbuckling of columns accounting for temperature effect on material properties," *J. Therm. Stress.*, vol. 45, no. 12, pp. 1043–1056, 2022. DOI: 10.1080/01495739.2022.2118198.

[18] V. Birman, "Vibrations of columns in the thermal postbuckling state accounting for temperature effect on material properties," *J. Therm. Stress.*, vol. 46, no. 11, pp. 1248–1265, 2023. DOI: 10.1080/01495739.2023.2232424.

[19] V. Birman, "Temperature effect on the properties and response of composite materials and plates," *AIAA J.*, vol. 62, pp. 1–12, 2024. DOI: 10.2514/1.J064367.

[20] Z. Jia, *et al.*, "An experimental investigation of the temperature effect on the mechanics of carbon fiber reinforced polymer composites," *Compos. Sci. Technol.*, vol. 154, pp. 53–63, 2018. DOI: 10.1016/j.compscitech.2017.11.015.

[21] M. M. Aghdam and S. R. Morsali, "Damage initiation and collapse behavior of unidirectional metal matrix composites at elevated temperatures," *Comput. Mater. Sci.*, vol. 79, pp. 402–407, 2013. DOI: 10.1016/j.commatsci.2013.06.024.

[22] J. M. Larsen, S. M. Russ and J. W. Jones, "An evaluation of fiber-reinforced titanium matrix composites for advanced high-temperature aerospace applications," *Metall. Mater. Trans. A*, vol. 26, no. 12, pp. 3211–3223, 1995. DOI: 10.1007/BF02669450.

[23] R. Leucht and H. J. Dudek, "Properties of SiC-fibre reinforced titanium alloys processed by fibre coating and hot isostatic pressing," *Mater. Sci. Eng. A*, vol. 188, no. 1-2, pp. 201–210, 1994. DOI: 10.1016/0921-5093(94)90373-5.

[24] Y. Li, *et al.*, "Temperature-dependent longitudinal tensile strength model for short-fiber-reinforced polymer composites considering fiber orientation and fiber length distribution," *J. Mater. Sci.*, vol. 53, no. 17, pp. 12190–12202, 2018. DOI: 10.1007/s10853-018-2517-8.

[25] J. H. Lou, *et al.*, "The analysis on transverse tensile behavior of SiC/Ti–6Al–4V composites by finite element method," *Mater. Des.*, vol. 31, no. 8, pp. 3949–3953, 2010. DOI: 10.1016/j.matdes.2010.03.034.

[26] G. M. Newaz and B. S. Majumdar, "A comparison of mechanical response of MMC at room and elevated temperatures," *Compos. Sci. Technol.*, vol. 50, no. 1, pp. 85–90, 1994. DOI: 10.1016/0266-3538(94)90128-7.

[27] S. Rahnama, R. Rafiee and M. Maleki, "The influence of hygrothermal environments on the stress concentration in unidirectional composite lamina," *Mech. Mater.*, vol. 129, pp. 332–340, 2019. DOI: 10.1016/j.mechmat.2018.12.010.

[28] M. G. Bader, "Tensile strength of uniaxial composites," *Sci. Eng. Compos. Mater.*, vol. 1, no. 1, pp. 1–12, 1988. DOI: 10.1515/SECM.1988.1.1.1.

[29] Y. Li, *et al.*, "Modeling the effects of interfacial properties on the temperature dependent tensile strength of fiber reinforced polymer composites," *Compos. Sci. Technol.*, vol. 172, pp. 74–80, 2019. DOI: 10.1016/j.compscitech.2019.01.011.

[30] W. A. Curtin, "Tensile strength of fiber-reinforced composites: III. Beyond the traditional Weibull model for fiber strengths," *J. Compos. Materi.*, vol. 34, no. 15, pp. 1301–1332, 2000. DOI: 10.1106/0GU5-LMTA-9R99-2W8K.

[31] W. A. Curtin, "Dimensionality and size effects on the strength of fiber-reinforced composites," *Compos. Sci. Technol.*, vol. 60, no. 4, pp. 543–551, 2000. DOI: 10.1016/S0266-3538(99)00150-5.

[32] I. M. Daniel, *et al.*, *Engineering Mechanics of Composite Materials*, vol. 3, New York: Oxford University Press, 1994.

[33] B. W. Rosen, N. F. Dow and Z. Hashin, "Mechanical properties of fibrous composites," National Aeronautics and Astronautics Administration, NASA-CR-31, 1964.

[34] W. Weibull, "A statistical distribution function of wide applicability," *J. Appl. Mech.*, vol. 18, no. 3, pp. 293–297, 1951. DOI: 10.1115/1.4010337.

[35] A. B. de Morais, "Prediction of the longitudinal tensile strength of polymer matrix composites," *Compos. Sci. Technol.*, vol. 66, no. 15, pp. 2990–2996, 2006. DOI: 10.1016/j.compscitech.2006.02.005.

[36] W. A. Curtin and S. J. Zhou, "Influence of processing damage on performance of fiber-reinforced composites," *J. Mech. Phys. Solids*, vol. 43, no. 3, pp. 343–363, 1995. DOI: 10.1016/0022-5096(94)00077-I.

[37] G. C. Foster, M. Ibnabdeljalil and W. A. Curtin, "Tensile strength of titanium matrix composites: direct numerical simulations and analytic models," *Int. J. Solids Struct.*, vol. 35, no. 19, pp. 2523–2536, 1998. DOI: 10.1016/S0020-7683(97)00148-0.

[38] S. B. Batdorf and R. Ghaffarian, "Tensile strength of unidirectionally reinforced composites—II," *J. Reinf. Plast. Compos.*, vol. 1, no. 2, pp. 165–176, 1982. DOI: 10.1177/073168448200100207.

[39] B. Budiansky, "Micromechanics," *Comput. Struct.*, vol. 16, no. 1-4, pp. 3–12, 1983. DOI: 10.1016/0045-7949(83)90141-4.

[40] B. Budiansky and N. A. Fleck, “Compressive kinking of fiber composites: A topical review,” *Appl. Mech. Rev.*, vol. 47, pp. S246–S250, 1994.
[41] B. W. Rosen, “Mechanics of composite strengthening,” in *Fiber Composite Materials, American Society of Metals.* Novelty, OH: Metals Park, 1965, pp. 37–75.
[42] A. S. Argon, *Treatise on Materials Science and Technology*, H. Herman, Ed., Vol. 1. New York: Academic Press, 1972.
[43] J. C. Halpin and J. L. Kardos, “Halpin-Tsai equations: a review,” *Polym. Eng. Sci.*, vol. 16, no. 5, pp. 344–352, 1976.
[44] C. L. Tucker, and E. Liang, “Stiffness predictions for unidirectional short-fiber composites: review and evaluation,” *Compos. Sci. Technol.*, vol. 59, no. 5, pp. 655–671, 1999. DOI: 10.1016/S0266-3538(98)00120-1.
[45] C. Leopold, *et al.*, “Comparison of analytical approaches predicting the compressive strength of fibre reinforced polymers,” *Materials*, vol. 11, no. 12, pp. 2517, 2018. DOI: 10.3390/ma11122517.
[46] L. S. Sutherland and C. Guedes Soares, “Review of probabilistic models of the strength of composite materials,” *Rel. Eng. Syst. Saf.*, vol. 56, no. 3, pp. 183–196, 1997. DOI: 10.1016/S0951-8320(97)00027-6.
[47] D. Liu, N. A. Fleck and M. P. F. Sutcliffe, “Compressive strength of fibre composites with random fibre waviness,” *J. Mech. Phys. Solids*, vol. 52, no. 7, pp. 1481–1505, 2004. DOI: 10.1016/j.jmps.2004.01.005.
[48] L. L. Vignoli, *et al.*, “Micromechanical analysis of transversal strength of composite laminae,” *Compos. Struct.*, vol. 250, pp. 112546, 2020. DOI: 10.1016/j.compstruct.2020.112546.
[49] L. Nicolais and R. A. Mashelkar, “The strength of polymeric composites containing spherical fillers,” *J. Appl. Polym. Sci*, vol. 20, no. 2, pp. 561–563, 1976. DOI: 10.1002/app.1976.070200226.
[50] L. E. Nielsen, “Simple theory of stress-strain properties of filled polymers,” *J Appl. Polym. Sci.*, vol. 10, no. 1, pp. 97–103, 1966. DOI: 10.1002/app.1966.070100107.
[51] F. Danusso and G. Tieghi, “Strength versus composition of rigid matrix particulate composites,” *Polymer*, vol. 27, no. 9, pp. 1385–1390, 1986. DOI: 10.1016/0032-3861(86)90038-8.
[52] S. S. Vel, “Exact thermoelastic analysis of functionally graded anisotropic hollow cylinders with arbitrary material gradation,” *Mech. Adv. Mater. Struct.*, vol. 18, no. 1, pp. 14–31, 2011. DOI: 10.1080/15376494.2010.519218.
[53] S. Ivanov, *et al.*, “Effect of elevated temperatures on the mechanical properties of a direct laser deposited Ti-6Al-4V,” *Materials*, vol. 14, no. 21, pp. 6432, 2021. DOI: 10.3390/ma14216432.
[54] H. M. Yun and J. A. DiCarlo, “Thermostructural Behavior of Sic Fiber Fabrics and Implications for Cmc,” in *24th Annual Conference on Composites, Advanced Ceramics, Materials, and Structures.B: Ceramic Engineering and Science Proceedings*. Hoboken, NJ: John Wiley & Sons, Inc, 2008, pp. 347–352.
[55] W.-S. Lee, C.-F. Lin and S. Z. Huang, “Effect of temperature and strain rate on the shear properties of Ti–6Al–4V alloy,” *Proc. Inst. Mech. Eng. C*, vol. 220, no. 2, pp. 127–136, 2006.
[56] P. J. Withers, J. A. Bennett and M. Kuroda, “Interfacial shear strength behaviour of Ti/SiC metal matrix composites at room and elevated temperature,” *Acta Mater.*, vol. 58, no. 18, pp. 6090–6103, 2010. DOI: 10.1016/j.actamat.2010.07.027.
[57] J. P. Favre, A. Vassel and C. Laclau, “Testing of SiC/titanium composites by fragmentation and push-out tests: comparison and discussion of test data,” *Composites*, vol. 25, no. 7, pp. 482–487, 1994. DOI: 10.1016/0010-4361(94)90173-2.
[58] M. D. Banea, L. F. M. D. Silva and R. Campilho, “Effect of temperature on tensile strength and mode I fracture toughness of a high temperature epoxy adhesive,” *J. Adhesion Sci. Technol.*, vol. 26, no. 7, pp. 939–953, 2012. DOI: 10.1163/156856111X593649.
[59] A. V. Movahedi-Rad and T. Keller, “A novel methodology of predicting temperature and rate effects on tensile properties of viscoelastic materials,” *Int. J. Non-Linear Mech.*, vol. 159, pp. 104613, 2024. DOI: 10.1016/j.ijnonlinmec.2023.104613.
[60] O. A. Plushchik and A. N. Aniskevich, “Effects of temperature and moisture on the mechanical properties of polyester resin in tension,” *Mech. Compos. Mater.*, vol. 36, no. 3, pp. 233–240, 2000. DOI: 10.1007/BF02681875.
[61] C. Alia, *et al.*, “Characterization of the chemical structure of vinyl ester resin in a climate chamber under different conditions of degradation,” *Polym. Degrad. Stab.*, vol. 153, pp. 88–99, 2018. DOI: 10.1016/j.polymdegradstab.2018.04.014.
[62] A. Plaseied* and A. Fatemi, “Strain rate and temperature effects on tensile properties and their representation in deformation modeling of vinyl ester polymer,” *Int. J. Polym. Mater.*, vol. 57, no. 5, pp. 463–479, 2008. DOI: 10.1080/00914030701729677.
[63] J. Hausmann and J. Schröder, *Compression Strength of Titanium Matrix Composites Depending on Fibre Volume Content, Fibre Orientation and Temperature*. Sendai, Japan: Japan Institute of Metals.